UC Irvine
Faculty Publications

Title

The influence of burn severity on postfire vegetation recovery and albedo change during early succession in North American boreal forests

Permalink

https://escholarship.org/uc/item/66x83398

Journal

Journal of Geophysical Research, 117(G1)

ISSN

0148-0227

Authors

Jin, Yufang
Randerson, James T.
Goetz, Scott J.
et al.

Publication Date

2012-03-01

DOI

10.1029/2011JG001886

Supplemental Material

https://escholarship.org/uc/item/66x83398#supplemental

Copyright Information

Peer reviewed

The influence of burn severity on postfire vegetation recovery and albedo change during early succession in North American boreal forests

Yufang Jin,[1] James T. Randerson,[1] Scott J. Goetz,[2] Pieter S. A. Beck,[2] Michael M. Loranty,[2] and Michael L. Goulden[1]

[1]   Severity of burning can influence multiple aspects of forest composition, carbon cycling, and climate forcing. We quantified how burn severity affected vegetation recovery and albedo change during early succession in Canadian boreal regions by combining satellite observations from the Moderate Resolution Imaging Spectroradiometer (MODIS) and the Canadian Large Fire Database. We used the MODIS-derived difference Normalized Burn Ratio (dNBR) and initial changes in spring albedo as measures of burn severity. We found that the most severe burns had the greatest reduction in summer MODIS Enhanced Vegetation Index (EVI) in the first year after fire, indicating greater loss of vegetation cover. By 5–8 years after fire, summer EVI for all severity classes had recovered to within 90%–108% of prefire levels. Spring and summer albedo progressively increased during the first 7 years after fire, with more severely burned areas showing considerably larger postfire albedo increases during spring and more rapid increases during summer as compared with moderate- and low-severity burns. After 5–7 years, increases in spring albedo above prefire levels were considerably larger in high-severity burns (0.20 ± 0.06; defined by dNBR percentiles greater than 75%) as compared to changes observed in moderate- (0.16 ± 0.06; for dNBR percentiles between 45% and 75%) or low-severity burns (0.13 ± 0.06; for dNBR percentiles between 20% and 45%). The sensitivity of spring albedo to dNBR was similar in all ecozones and for all vegetation types along gradients of burn severity. These results suggest carbon losses associated with increases in burn severity observed in some areas of boreal forests may be at least partly offset, in terms of climate impacts, by increases in negative forcing associated with changes in surface albedo.

1.   Introduction

[2]   Fire is the primary driver of the North American boreal region vegetation dynamics [*McGuire et al.*, 2004], carbon cycling [*Balshi et al.*, 2007; *Bond-Lamberty et al.*, 2007; *Balshi et al.*, 2009], and surface energy exchange [*Chambers and Chapin*, 2002; *Liu et al.*, 2005; *Amiro et al.*, 2006; *Lyons et al.*, 2008; *Rocha and Shaver*, 2011], by altering vegetation structure, albedo, surface temperature, and evapotranspiration. The integrated net effect of these processes is a positive transient forcing of climate during the first decade after fire from greenhouse gas emissions,

followed by a small negative forcing in subsequent decades due to persistent increases in spring and summer surface albedo and carbon uptake by regrowing forests [*Randerson et al.*, 2006]. The balance between positive and negative forcing at a landscape scale depends on changes in the fire regime, including area burned and burn severity, as well as processes that influence postfire succession. Changes in the boreal fire regime have the potential to substantially influence carbon fluxes and regional to global climate on multidecadal to century timescales [*Bonan et al.*, 1992; *McGuire et al.*, 2004; *Randerson et al.*, 2006; *Zhuang et al.*, 2006; *Flanner et al.*, 2007; *Euskirchen et al.*, 2009].

[3]   The North American boreal region fire regime has been intensifying since the 1970s, a trend that is expected to accelerate in response to future climate change [*Flannigan et al.*, 2005]. A pronounced upward trend in total burned area was observed in Canada during 1959–1999 [*Flannigan et al.*, 2000], mostly due to longer and warmer fire seasons

---

[1]Department of Earth System Science, University of California, Irvine, California, USA.
[2]Woods Hole Research Center, Falmouth, Massachusetts, USA.

[*Wotton and Flannigan*, 1993; *Gillett et al.*, 2004]. Given projections of climate change over the next several decades, 10 year mean burned area may double by 2041–2050 relative to 1991–2000, and increase by as much as 3.5–5.5 times by 2091–2100 [*Balshi et al.*, 2009; *Krawchuk and Cumming*, 2011]. Increases in fire extent are likely to be accompanied by increases in burn severity [*Duffy et al.*, 2007], which is commonly defined in boreal forests as the proportion of forest floor and soil organic matter consumed by fire [*de Groot et al.*, 2009]. In turn, increasing fire severity may have important effects on carbon cycling and postfire trajectories of ecosystem recovery [*Goetz et al.*, 2007; *French et al.*, 2008; *Mack et al.*, 2008]. Burn severity in the Alaskan boreal forest increases month by month through the fire season, and may be higher during large fire years [*Kasischke and Turetsky*, 2006; *Duffy et al.*, 2007; *Turetsky et al.*, 2011a].

[4] Changes in burn severity have the potential to modify regional and global climate in ways that may amplify or offset effects associated solely with regional changes in burned area. Burn severity influences both the amount of carbon emitted immediately during the fire event and the rates of long-term carbon reaccumulation within the burn perimeter [*Kurz and Apps*, 1999; *Harden et al.*, 2000; *Conard et al.*, 2002; *Balshi et al.*, 2007]. Especially severe fires emit more aerosols and greenhouse gases, but also modify postfire trajectories of species composition and rates of carbon accumulation [*Johnstone and Chapin*, 2006; *Beck et al.*, 2011]. Although the North American boreal forest fires are predominantly stand-replacing, high-intensity crown fires [*Johnson et al.*, 1998], the soil organic material can burn to varying depths, and thus fire creates substantial heterogeneity in soil burn severity at patch and landscape scales [*Miyanishi and Johnson*, 2002]. Variations in burn severity can influence soil thermal and hydraulic properties by affecting the organic layer depth, and thus soil moisture and temperature [*Yi et al.*, 2009]. These changes in soil physical properties and microclimate, in turn, influence the recruitment and establishment of trees within the burn perimeter [*Johnstone and Chapin*, 2006; *Johnstone et al.*, 2010; *Shenoy et al.*, 2011]. Increases in both burned area and severity have accelerated regional carbon losses over the past decade in Alaskan black spruce stands, and as a result, soils have been a net source of carbon to the atmosphere, with carbon emissions exceeding uptake in unburned stands [*Turetsky et al.*, 2011a].

[5] Most information on postfire succession in the boreal region to date comes from chronosequence studies comparing communities of different ages [*Mack et al.*, 2008; *Goulden et al.*, 2011], or direct observations of postfire tree densities [*Johnstone and Kasischke*, 2005; *Shenoy et al.*, 2011]. A large pulse of postfire tree recruitment appears shortly after fire, followed by several decades with minimal recruitment [*Johnstone et al.*, 2004]. Studies show that burn severity has a strong positive effect on seed germination and net seedling establishment after 3 years in the North American boreal region, due to exposed mineral soil and reduced moisture stress after severe burning [*Lavoie and Sirois*, 1998; *Johnstone et al.*, 2004]. Severe fire exposes more and deeper mineral soil, which favors the recruitment of deciduous species and decreases the relative abundance of black spruce in the first decade after fire [*Johnstone and*

Chapin, 2006; *Johnstone et al.*, 2010; *Kasischke et al.*, 2010]. The initial effect of postfire organic layer depth on deciduous recruitment is likely to translate into a prolonged phase of deciduous dominance during postfire succession in severely burned stands [*Shenoy et al.*, 2011], supporting the hypothesis that early establishment patterns are a key regulator of stand composition in midsuccessional stands.

[6] Several field and remote sensing studies have characterized the effects of fire on surface albedo. Winter and spring albedos typically increase after fire as a result of loss of canopy overstory and greater exposure of snow-covered surfaces [*Liu et al.*, 2005; *Amiro et al.*, 2006; *Lyons et al.*, 2008]. In contrast, postfire summer albedo is typically reduced for several years as a consequence of black carbon coatings on soils and the boles of dead trees [*Chambers and Chapin*, 2002]. Establishment and growth of herbaceous plants, shrubs, and deciduous trees cause rapid increases in summer albedo within the first decade after fire [*Lyons et al.*, 2008; *McMillan and Goulden*, 2008]. Less is known about the role of burn severity in determining postfire changes in surface albedo and energy exchange [e.g., *Rocha and Shaver*, 2011], particularly during the first few decades after fire in boreal forests. Midsuccessional stands that experienced more severe burns have been shown to have consistently higher winter and spring albedos as a consequence of a greater deciduous tree cover [*Beck et al.*, 2011]. Local cooling may be further enhanced in these deciduous stands as a consequence of greater partitioning of energy into latent heat flux due to higher stomatal and canopy conductance during summer, as compared to conifer stands [*Baldocchi et al.*, 2000; *Eugster et al.*, 2000; *Bond-Lamberty et al.*, 2009].

[7] The objective of this study was to quantify and understand the impacts of burn severity on vegetation recovery and albedo within the first decade after fires in four major ecozones in Canada. We tested the hypothesis that more severe fires caused faster vegetation recovery and larger postfire albedo increases than less severe fires as a consequence of the relationship between burn severity and postfire species establishment [*Johnstone and Kasischke*, 2005; *Johnstone and Chapin*, 2006; *Johnstone et al.*, 2010].

2. Materials and Methods

[8] Measures of burn severity, vegetation productivity, and albedo were derived from Moderate Resolution Imaging Spectroradiometer (MODIS) satellite observations. We used two measures of burn severity: the difference Normalized Burn Ratio (dNBR) and the initial spring albedo change ($\Delta\alpha_0$), described below. Dynamics of vegetation recovery and albedo during early succession were analyzed for three burn severity classes as well as along continuous gradients of dNBR and $\Delta\alpha_0$.

2.1. Boreal Ecozones and Vegetation Types

[9] The study area is central west Canada (50°N~70°N, 140°W~80°W), where we focused on four major ecozones: boreal plains, boreal shield west, taiga plains, and taiga shield west (Figure 1a) [*Marshall et al.*, 1999]. Boreal plains are to the north of the prairie ecozone, with black spruce (*Picea mariana*) and tamarack (*Larix laricina*) commonly found in the north, and aspen (*Populus tremuloides*) and
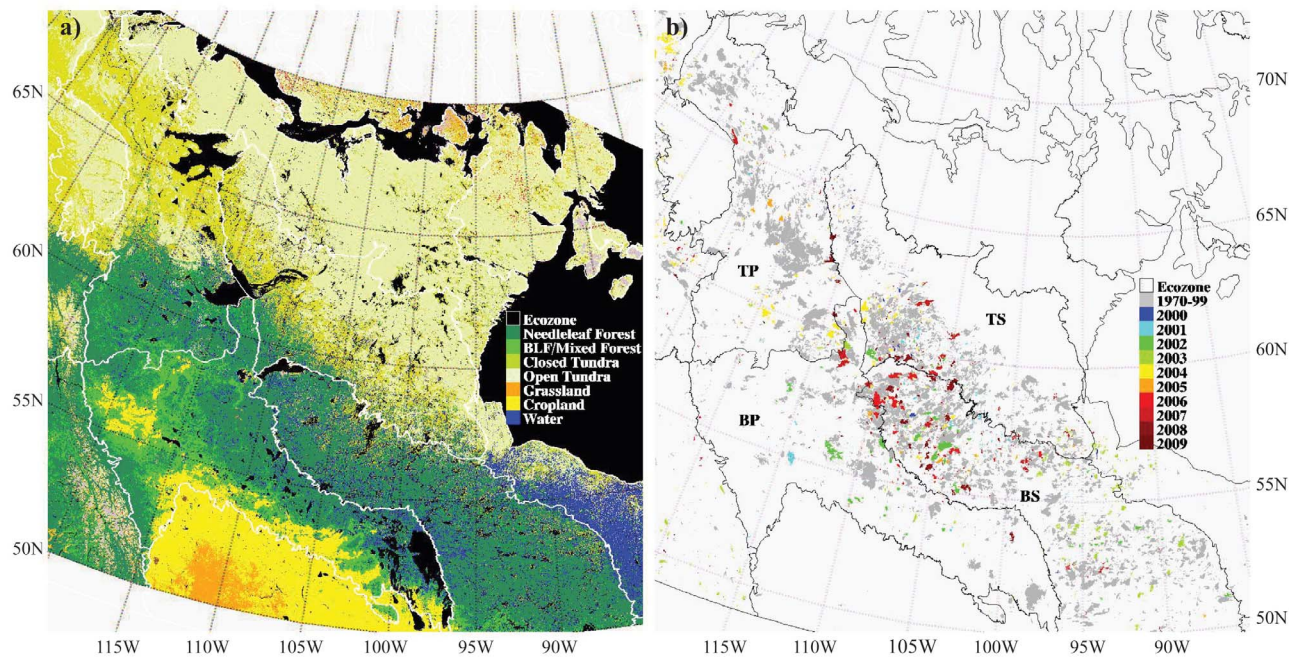
Figure 1. Maps of the study area showing (a) boreal ecozones superimposed on MODIS land cover types and (b) the area burned during 2000–2009. Only fires greater than 100 ha were included in our analysis, and a 500 m inside buffer was applied prior to sampling Moderate Resolution Imaging Spectroradiometer (MODIS) data within burn perimeters. The closed shrublands class included closed shrublands and woody savannas identified by MODIS International Geosphere-Biosphere Programme (IGBP) product. The open shrublands class was composed mostly of open shrublands. Four major ecozones analyzed here include boreal plains (BP), boreal shield (BS), taiga plains (TP), and taiga shield (TS).

balsam poplar (*Populus balsamifera*) more abundant in the south. Boreal shield, which is east of boreal plains, is the largest Canadian ecozone, dominated by closed-canopy black and white spruce (*Picea glauca*), balsam fir (*Abies balsamea*), and tamarack. Taiga plains are low-lying plains at the northern edge of boreal coniferous forest, with open black spruce stands intermixed with shrub and tundra ecosystems, and lichens and moss ground cover. Taiga shield is

to the east of taiga plains and north of boreal shield, covered by a patchwork of rock outcrops, open lichen forest stands (composed of small black spruce, alder, willow and larch), and shrublands. Western mountain regions were not included in this study because they experienced fewer fires than the four ecozones studied here, and their complex topography reduced the accuracy of the MODIS albedo retrievals.

Table 1. Vegetation Characteristics in the Study Area

	Boreal Plains	Boreal Shield	Taiga Plains	Taiga Shield
Total land (number of 500 m pixels)[a]	2,518,681	2,295,327	2,163,738	2,100,836
Burned area (%)[b]	12	32	23	22
Nonburned areas (number of 500 m pixels)[c]	1,795,663	1,225,083	1,376,201	1,438,298
Percentage of land cover types				
Needleleaf forest[d]	56	92	49	12
Broadleaf/Mixed forest[d]	20	3	2	0
Closed shrublands[d]	1	4	25	22
Open shrublands[d]	0	0	24	66
Others[d]	22	0	0	0
Mean summer EVI[e]				
Needleleaf forest	0.38	0.33	0.35	0.27
Broadleaf/mixed forest	0.51	0.44	0.49	–
Closed shrublands	0.39	0.30	0.30	0.25
Open shrublands	0.42	0.32	0.32	0.28
All (±std)	0.43 (±0.08)	0.33 (±0.06)	0.33 (±0.07)	0.27 (±0.06)

[a]Lakes and rivers were excluded, and only 500 m land pixels were counted.
[b]Percent of land areas burned during 1970–2009 based on the Canadian Large Fire Database (LFDB).
[c]Areas that were not burned during 1950–2009 according to LFDB; 1 km outside buffer was applied; lakes and rivers were excluded.
[d]Land cover type for each 500 m pixel was based on the most frequent vegetation type during 2001–2009 identified from annual Moderate Resolution Imaging Spectroradiometer (MODIS) 500 m land cover product (MCD12Q1) [*Friedl et al.*, 2002].
[e]Summer Enhanced Vegetation Index (EVI) was averaged during 2000–2009 in the nonburned areas for days of year 177–224.

Table 2. Characteristics of the Areas Burned Averaged During 2001–2009

	Boreal Plains	Boreal Shield	Taiga Plains	Taiga Shield
Burned Area Statistics				
Number of fire polygons (greater than 100 ha)	207	588	197	354
Burned area (10^6 ha)	1.75	4.57	1.46	2.02
Number of 500 m pixels[a]	41,397	105,415	33,282	47,067
Percentage of Prefire Vegetation Types[b]				
Needleleaf forest	71%	59%	30%	24%
Broadleaf/Mixed forest	13%	3%	1%	1%
Closed shrublands	8%	26%	56%	64%
Open shrublands	1%	5%	10%	9%
Others	6%	8%	3%	2%
EVI Characteristics				
Summer EVI (prefire)[d]	0.35 (±0.08)	0.29 (±0.06)	0.31 (±0.05)	0.27 (±0.05)
Summer EVI change (first year after fire)[c]	−0.10 (±0.06)	−0.12 (±0.06)	−0.12 (±0.05)	−0.12 (±0.05)
Burn Severity Metrics[c]				
Difference Normalized Burn Ratio (dNBR)	0.35 (±0.17)	0.42 (±0.17)	0.35 (±0.14)	0.41 (±0.16)
Summer NBR (prefire)[d]	0.58 (±0.09)	0.50 (±0.10)	0.49 (±0.06)	0.44 (±0.07)
Summer NBR (first year after fire)[d]	0.24 (±0.20)	0.08 (±0.18)	0.14 (±0.15)	0.03 (±0.15)
Spring albedo (prefire)[d]	0.27 (±0.08)	0.28 (±0.07)	0.32 (±0.08)	0.30 (±0.07)
Spring albedo change (first year after fire)[c]	0.10 (±0.06)	0.10 (±0.06)	0.10 (±0.06)	0.10 (±0.05)
Correlation between prefire NBR and dNBR	−0.01	0.18	0.07	0.30
Correlation between postfire NBR and dNBR	−0.89	−0.86	−0.91	−0.89
Correlation between prefire EVI and dNBR	−0.35	−0.20	−0.02	−0.17
Correlation between EVI change and dNBR[d]	−0.74	−0.69	−0.78	−0.68

[a]Only pixels within 500 m inside buffer of fire polygons and outside of 1 km buffer of rivers and lakes were retained for analysis.
[b]Percent of prefire vegetation types were based on the annual MODIS 500 m land cover product before fire.
[c]Change here refers to difference between the year after fire and the year before fire.
[d]Summer is defined as a time period for days of year 177–224, and spring is defined as a time period for days of year 49–96.

[10] We used the collection 5 MODIS yearly land cover product at 500 m resolution for 2001–2009 (MCD12Q1) to characterize the land cover type for unburned areas and to identify the preburn land cover type [*Friedl et al.*, 2002, 2010]. We aggregated the closed shrublands and woody savannas to one class based on their similarity in the fractional coverage of woody plants; we hereafter refer to this lumped class as closed shrublands. We analyzed the dominant land cover type during 2001–2009 for each pixel in areas that were not burned since 1950 (>1 km outside fire perimeters; see section 2.2). Needleleaf forest dominated the boreal plains, boreal shield, and taiga plains, occupying 56%, 92%, and 49% of nonburned land areas, respectively (Table 1); broadleaf and mixed forests were only significant in boreal plains (20%) and decreased from south to north and from west to east. Closed and open shrublands both occupied approximately 25% of nonburned areas in taiga plains. Open shrublands dominated taiga shield, accounting for 66% of the land cover in this ecoregion.

2.2. Fire History

[11] We used the Canadian Large Fire Database (LFDB) from the Canadian Forest Service (available at http://cwfis. cfs.nrcan.gc.ca/en_CA/datamart, accessed 10 January 2012) to identify the year and location of fires during 1950–2009 [*Stocks et al.*, 2002] (Figure 1b). The LFDB is a compilation of forest fire data from all Canadian agencies, including provinces, territories, and Parks Canada. The data set accounts for more than 97% of the total area burned on average [*Amiro et al.*, 2001; *Stocks et al.*, 2002]. Different provinces had records available for different time periods. Manitoba and Saskatchewan data, for example, were

available starting, respectively, in 1980 and 1945. We extracted fires greater than 100 ha that occurred between 2001 and 2009, and applied a 500 m inside buffer to avoid the uncertainties in georegistration and fire perimeter delineation [*Goetz et al.*, 2006]. A total of 1346 fires (polygons) during 2001–2009 were analyzed, comprising a total burned area of 9.79 million ha (Table 2 and, in Text S1 in the auxiliary material, Table S1).[1] Boreal shield had the most fires (n = 588) and largest burned area (4.57 million ha); taiga shield had the second largest number of fires (n = 354) and a burned area of 2.02 million ha. Interannual variability in burned area was considerable during 2001–2009; burned area was highest during 2002 and lowest during 2009 (Table S1 in Text S1). We also identified unburned areas by masking all fires since 1950, expanded by a 1 km outside buffer.

2.3. MODIS Enhanced Vegetation Index and Albedo

[12] Vegetation indices (VI) from satellite observed surface reflectance at two or more spectral bands highlight the presence and abundance of vegetation in the landscape and allow spatial and temporal comparisons of vegetation productivity [*Tucker and Sellers*, 1986; *Goetz and Prince*, 1998]. The Enhanced Vegetation Index (EVI) is a modified version of the normalized difference vegetation index that includes adjustments for canopy background and residual atmospheric contamination using blue band surface reflectance [*Huete et al.*, 2002]. EVI is highly correlated with gross primary productivity in both evergreen

___
[1]Auxiliary materials are available in the HTML. doi:10.1029/2011JG001886.
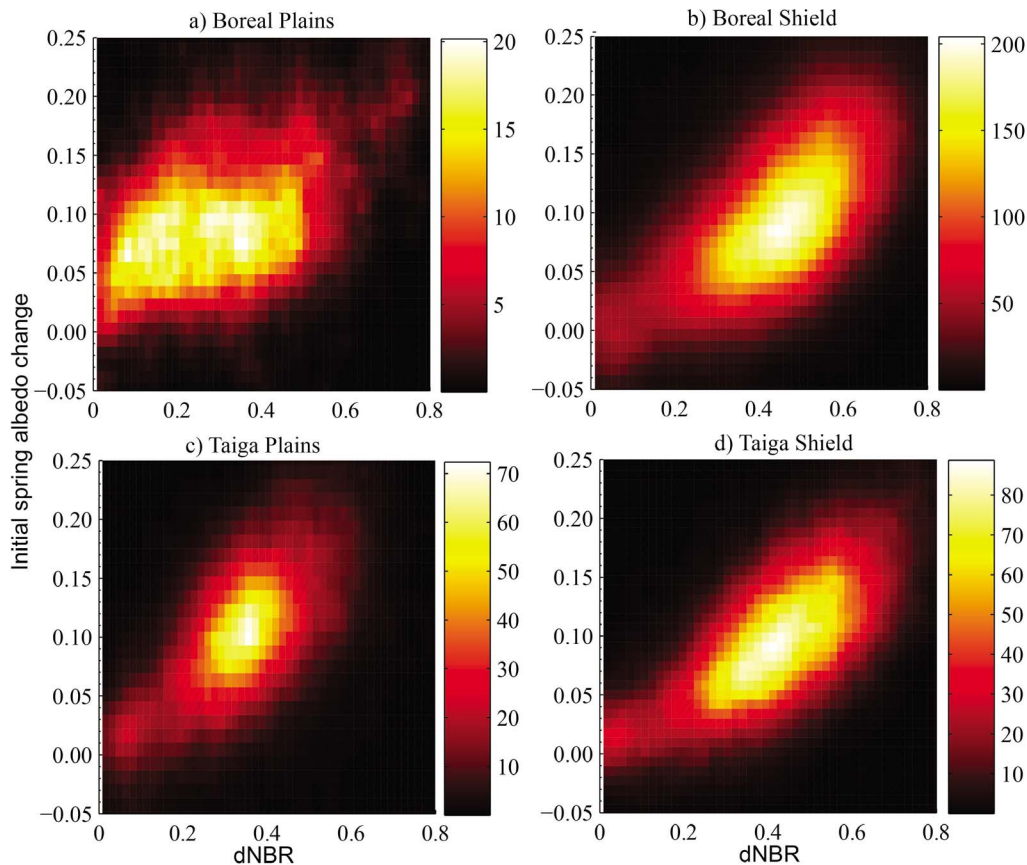
Figure 2. Density plots of initial shortwave spring albedo change ($\Delta\alpha_0$) (1 year after fire – 1 year after fire) versus difference Normalized Burn Ratio (dNBR). Spring albedo was averaged for days of year 49–96. Both dNBR and $\Delta\alpha_0$ were divided to 50 bins.

needleleaf forests and deciduous broadleaf forest [*Xiao et al.*, 2004a, 2004b; *Rahman et al.*, 2005; *Sims et al.*, 2006; *McMillan and Goulden*, 2008]. Here we used 16 day EVI data during 2000–2011 from the collection 5 Terra MODIS 500 m VI product (MOD13A1) [*Huete et al.*, 2002] to analyze postfire vegetation dynamics. Over the nonburned areas of the four ecozones, boreal plains had the highest mean midsummer EVI during 2000–2009 (0.43 ± 0.08), followed by both boreal shield and taiga plains (0.33 ± 0.06), and taiga shield (0.27 ± 0.06) (Table 1). Within the nonburned needleleaf forest, the highest EVI was observed in boreal plains while the lowest in taiga shield.

[13] For albedo we used the MODIS collection 5 product at 500 m resolution (MCD43A3) for 2000–2011 [*Schaaf et al.*, 2002; *Jin et al.*, 2003]. Both Terra and Aqua data are used in this product to provide more diverse angular samplings and increased probability of high-quality input data allowing more accurate bidirectional reflectance distribution function (BRDF) and albedo retrievals. If the majority of the surface reflectance observations during a 16 day period have characteristics consistent with snow cover, the snow-free observations are discarded during construction of the BRDF and the retrieval is flagged as "snow" in the corresponding quality product (MCD43A2) (MCD43 user's guide, available at http://www.modis.bu.edu/brdf/userguide/intro.html)

[*Jin et al.*, 2002]. White sky albedo is an integration of BRDF over both incoming and outgoing hemispheres and does not depend on the illumination and atmospheric condition. In our analysis we used the white sky albedo in the total shortwave (SW) spectrum (0.3–5.0 μm). We retained only MODIS data of the highest quality, based on the BRDF and albedo quality product (MCD43A2). Full BRDF model inversions (full inversion) are made when a sufficient number of high-quality directional observations are available to adequately sample the BRDF and to achieve the highest accuracy [*Schaaf et al.*, 2002].

2.4. Burn Severity

[14] Normalized Burn Ratio (NBR) and differenced Normalized Burn Ratio (dNBR) [*Key and Benson*, 2006] have been widely used as a measure of burn severity from satellite observations [*French et al.*, 2008]. NBR is defined as the difference between near and shortwave infrared reflectance, normalized by the sum of the reflectance measured at these two wavelengths. dNBR, defined as NBR$_{prefire}$ − NBR$_{postfire}$, is positively correlated with field measurements of burn severity in both Alaska and western Canada [*Epting et al.*, 2005; *Allen and Sorbel*, 2008; *Hall et al.*, 2008; *Soverel et al.*, 2010]. We used the spectral white sky albedos for MODIS band 2 (841–876 nm) and band 7 (2105–2155 nm)

Table 3. Sensitivities of Albedo Before Fire, 1 Year After Fire, and 5–7 Years After Fire and Albedo Change (5–7 Years After Fire) to dNBR in Each Ecozone[a]

	Prefire Albedo			Initial Albedo Change[b]			Albedo (5–7 Years)			Albedo Change (5–7 Years)		
	r	b	ci	r	b	ci	r	b	ci	r	b	ci
Summer												
Boreal plains	−0.54	−0.06	0.001	−0.44	−0.03	0.001	−0.51	−0.07	0.001	0.01	0.00	0.001
Boreal shield	−0.32	−0.03	0.001	−0.39	−0.03	0.000	−0.16	−0.01	0.001	0.26	0.02	0.000
Taiga plains	−0.28	−0.02	0.001	−0.55	−0.04	0.001	−0.08	−0.01	0.001	0.26	0.02	0.001
Taiga shield	−0.39	−0.03	0.001	−0.53	−0.03	0.001	−0.29	−0.03	0.001	0.32	0.02	0.001
Spring												
Boreal plains	−0.40	−0.17	0.009	0.46	0.15	0.007	0.04	0.02	0.015	0.61	0.31	0.012
Boreal shield	−0.34	−0.14	0.003	0.61	0.22	0.003	0.38	0.17	0.003	0.72	0.32	0.003
Taiga plains	−0.22	−0.13	0.010	0.61	0.27	0.006	0.33	0.21	0.010	0.66	0.35	0.006
Taiga shield	−0.45	−0.20	0.005	0.67	0.23	0.003	0.20	0.08	0.006	0.71	0.29	0.004

[a]Here r, correlation coefficient; b, slope; and ci, 95% confidence interval for the linear regression slope of albedo versus dNBR.
[b]Initial albedo change refers to the difference of albedo between 1 year after fire and 1 year before fire.

to calculate NBR during the summer (the last week of June to the second week of August, days of year 177–224), for each year. dNBR was then calculated at 500 m resolution for all pixels burned since 2001 by subtracting summer NBR a year after fire from that a year before fire.

[15] Some studies indicate that dNBR may not always adequately capture the depth of burning into the surface organic soil in some areas [*French et al.*, 2008; *Hoy et al.*, 2008; *Kasischke et al.*, 2008; *Barrett et al.*, 2010]. We therefore developed an alternative measure of burn severity using initial SW spring albedo change ($\Delta\alpha_0$). We calculated $\Delta\alpha_0$ during periods of snow cover for days of year 49–96 from a year after fire and a year before fire. Deeper burning of organic soils may weaken or damage supporting roots for dead boles and thus cause more dead trees to fall [e.g., *Bond-Lamberty and Gower*, 2008]. Losses in canopy overstory and fallen dead boles associated with more severe fires [*Kasischke et al.*, 2000] would be expected to allow more exposure of snow-covered surfaces during early spring, and thus higher levels of SW albedo measured by MODIS. A relatively high correlation between dNBR and $\Delta\alpha_0$ provided evidence that this was a reasonable alternate measure of severity (Figure 2 and Table 3). Indirect evidence for the use of $\Delta\alpha_0$ as a severity metric comes from postfire trajectories that show progressive decreases in spring albedo during two to five decades after fire, a period when the growth of deciduous and conifer trees would be expected to reduce the exposure of surface snow [*Lyons et al.*, 2008].

2.5. Trajectories of Postfire EVI and Albedo

[16] We stratified the 500 m data to three classes of burn severity, based on dNBR and initial albedo change ($\Delta\alpha_0$) histograms, separately. For each ecozone, dNBR (or $\Delta\alpha_0$) values between 20%–45%, 45%–75% and >75% percentiles were assigned to low, moderate, and high severity classes, respectively. We aggregated the annual time series of summer EVI (days of year 177–224) during 2000–2011 to build average postfire trajectories according to the fire year and the year of satellite observations, for each severity class in each ecozone. The trajectories were cut off at 8 years after fire to assure that each postfire year included diverse areas burned in 3 or more different years. EVI at 1 year before fire and a prefire EVI climatology (averaged over all available
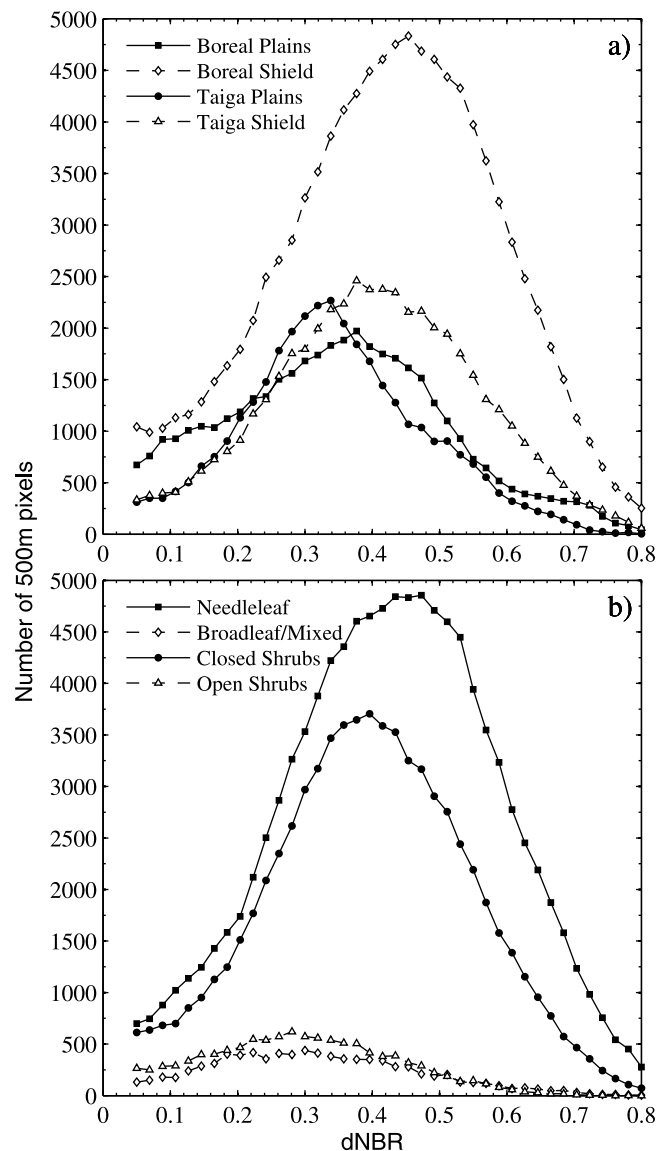
Figure 3. Histograms of dNBR for all areas burned during 2001–2009 for (a) each ecozone and (b) each vegetation type.
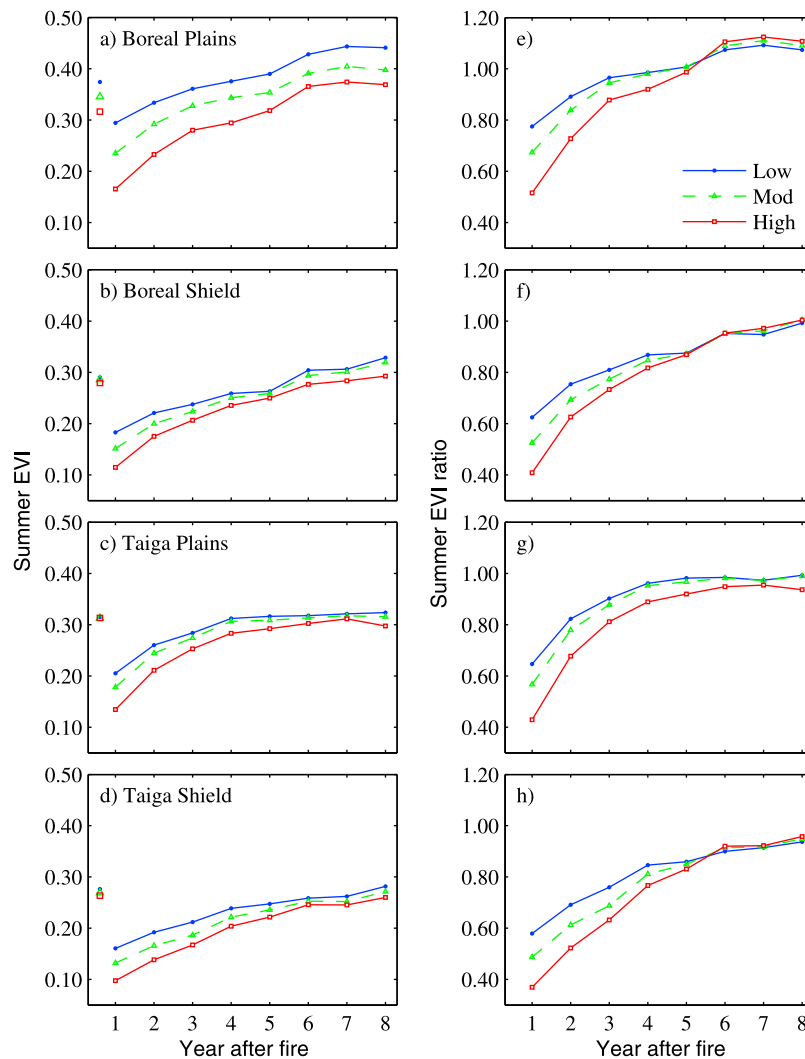
Figure 4. Trajectories of (a–d) summer Enhanced Vegetation Index (EVI) and (e–h) EVI ratio (postfire divided by prefire) for low, moderate, and high burn severity classes. Summer EVI was averaged for days of year 177–224. The prefire EVI means are shown with individual symbols in Figures 4a–4d on the x axis before the first year after fire.

years before fire) were also calculated for each severity class.

[17] Similar aggregation was done to build postfire trajectories for summer albedo (days of year 177–224) and spring albedo (days of year 49–96). We extracted the best quality (full inversion) albedo retrievals under snow conditions for the spring albedo time series. Figure S1 in Text S2 shows that the accumulated number of pixels for the trajectories decreased with year since fire. For spring albedo trajectories, we only included data for up to 7 years after fire since not all ecozones had more than 500 pixels with valid albedo data from the eighth postfire year. We also summarized the data at 1 year after fire, and averaged 5–7 years after fire for each dNBR and $\Delta\alpha_0$ increment, to analyze the sensitivity of vegetation and albedo change to burn severity. A prefire albedo climatology also was calculated for each corresponding dNBR and $\Delta\alpha_0$ increment. The number of 500 m pixels with high-quality albedo observations during

summer and spring as a function of dNBR and $\Delta\alpha_0$ increment are shown in Figures S2 and S3 (Text S2).

3. Results

3.1. Characteristics of Burn Severity

[18] Burn severity varied considerably within and across the boreal ecozones (Figure 3a and Table 2). Boreal shield and taiga shield had higher average dNBR values (0.42 ± 0.17) than boreal plains (0.35 ± 0.17) and taiga plains (0.35 ± 0.14). The majority of land burned during 2002–2009 was classified as needleleaf forest before fire by the MODIS land cover product [*Friedl et al.*, 2010], followed by closed shrublands (Figure 3b and Table 2). Boreal needleleaf forest had the highest dNBR (0.42 ± 0.18), followed by closed shrublands (0.39 ± 0.17). Broadleaf/mixed forests and open shrublands had the lowest dNBR (0.27 ± 0.19). The distribution of fire pixels as a function
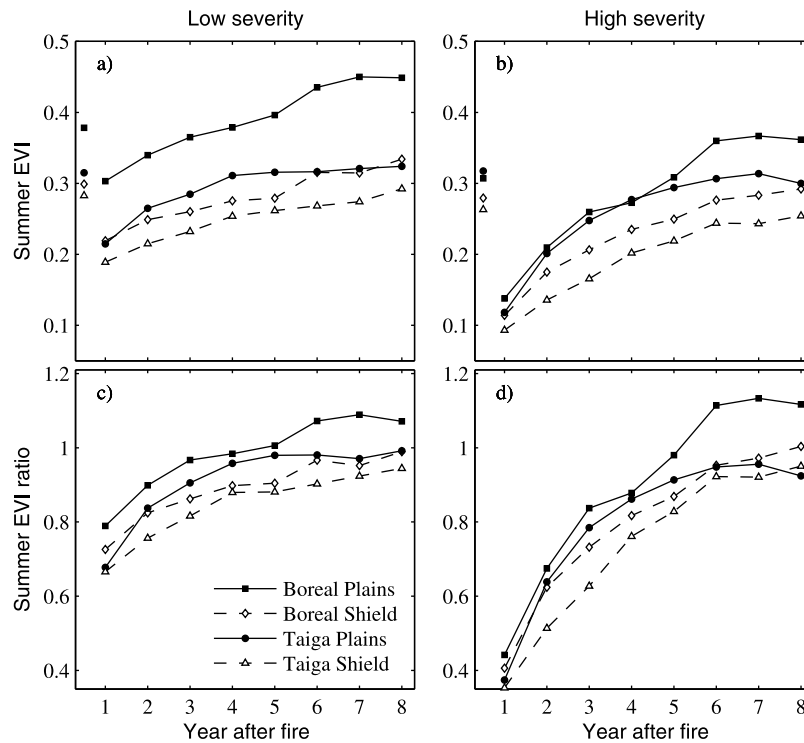
Figure 5. Trajectories of (a and b) summer EVI values across ecozones and (c and d) EVI ratio (postfire/prefire) for low and high burn severity classes derived using dNBR thresholds from *Epting et al.* [2005] and *Hall et al.* [2008]. The same dNBR thresholds were used to stratify burned areas for all ecozones, with dNBR values of 0.17–0.32 for low severity and dNBR values of 0.55–0.98 for high severity.

of burn severity for different ecozones and land cover types was similar when $\Delta\alpha_0$ was used as the burn severity metric (Figure S4 in Text S2).

[19] dNBR in each ecozone was mainly controlled by postfire NBR values. Postfire NBR had large variations within and across ecozones and explained 74%–83% of variance in dNBR, while prefire NBR varied much less and explained only 0%–4% of dNBR variance (9% in taiga shield) (Table 2 and Figure S5 in Text S2). This provides evidence that for NABR, our dNBR observations were most sensitive to the status of the postfire land surface, including the forest canopy and floor. Lower correlation between prefire EVI and dNBR further confirmed this (r = −0.02 − −0.20 except for boreal plains where r = −0.35) (Figure S6 in Text S2 and Table 2). In contrast, dNBR was strongly negatively correlated with the initial summer EVI change (r = −0.68 − −0.78) (Table 2 and Figure S7 in Text S2), which was expected as both dEVI and dNBR are sensitive to change in near infrared reflectance.

3.2. Effects of Burn Severity on Postfire EVI Recovery

[20] Summer EVI decreased 1 year after fire due to the removal of overstory and understory vegetation (Figure 4 and Table S2 in Text S1). The most severe burns had the greatest initial EVI reduction and the lowest summer EVI 1 year after fire (Figure 4). The EVI reduction ranged from 0.08 in boreal plains to 0.12 in taiga shield for low-severity burns, and from 0.15 in boreal plains to 0.18 in taiga plains for high-severity burns. The standard deviation of the EVI reduction was less than 0.04 for all burn severity classes. EVI after 1 year was significantly lower (student's *t* test,

df >= 17466, p < 0.0001, H_1: $EVI_{low\_severity} > EVI_{high\_severity}$) in the most severe burns compared to low-severity burns (Table S2 in Text S1). Summer EVI before fire was similar for the various burn severity classes (two-tailed student's *t* test, df >= 17499, p < 0.0001, H_0: $EVI_{low\_severity} = EVI_{high\_severity}$). The differences of initial postfire EVI values and EVI decreases among burn severity classes were therefore primarily a consequence of severity as opposed to differences in prefire vegetation.

[21] EVI increased rapidly during the first 2 to 4 years after fire, probably as a result of the establishment and growth of herbaceous species and shrubs (Figure 4). The recovery rates of EVI, defined as the annual increase of summer EVI from the initial postfire EVI, were generally faster for the most severe burns than for low-severity burns during this time (Figures 4e–4h). As a consequence, by 5–8 years after fire, EVI from areas with varying levels of burn severity had mostly converged, and were between 90% and 108% of prefire values (Figures 4e–4h). When burn severity classes were derived from initial spring albedo change ($\Delta\alpha_0$), a parallel analysis yielded similar postfire EVI trajectories (Figure S8 in Text S2).

[22] Boreal plains had the fastest vegetation recovery for both low- and high-severity fires, i.e., summer EVI was higher than prefire EVI by 6 years after fire (df = 6378, p < 0.0001, H_0: $EVI_{6y} = EVI_{prefire}$) (Figure 4). Taiga shield had the slowest recovery, where summer EVI was still significantly lower than the prefire EVI by 8 years after fire (df = 2751, p < 0.0001, H_0: $EVI_{8y} = EVI_{prefire}$). When the data were stratified into just two burn severity classes with the same dNBR thresholds used by *Epting et al.* [2005] and
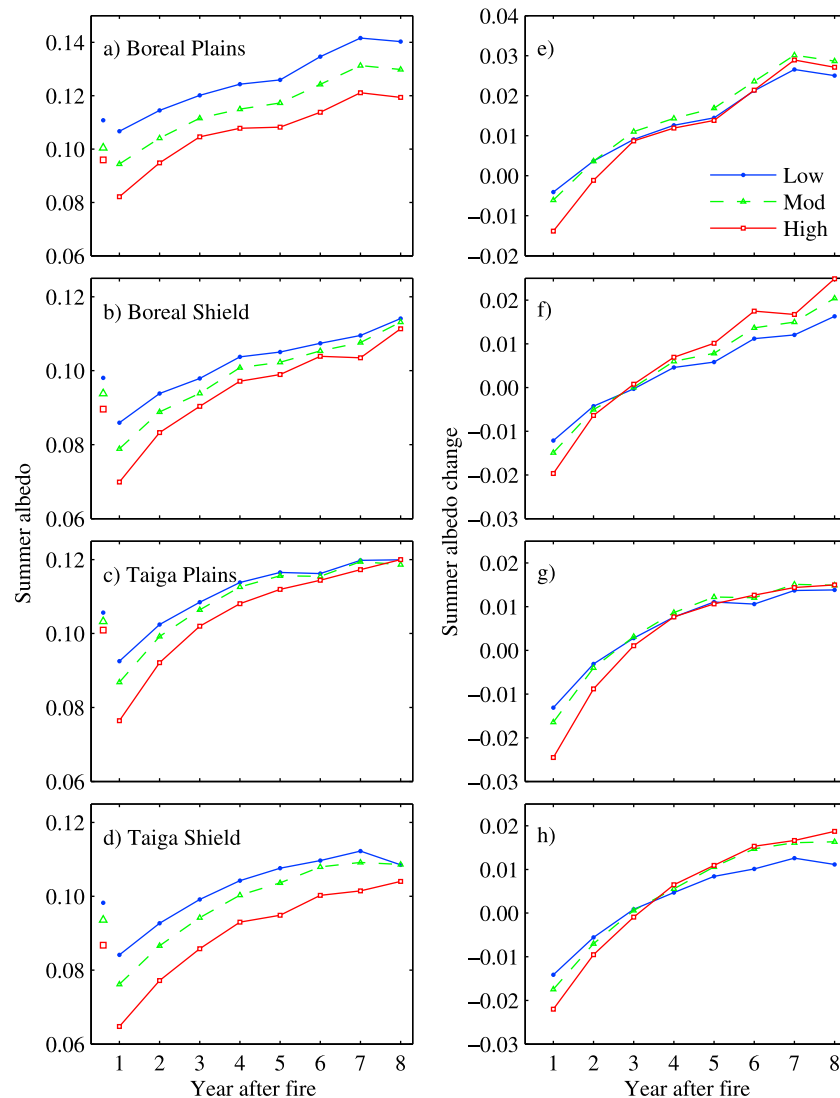
Figure 6. Trajectories of (a–d) summer albedo and (e–g) summer albedo change for each burn severity class stratified based on dNBR histograms in each ecozone. The prefire albedo means are shown with individual symbols in Figures 6a–6d on the x axis before the first year.

Hallet al. [2008], similar EVI results were found across ecozones and among severity classes (Figure 5). This comparison indicated that our results related to the effect of burn severity on postfire trajectory were not dependent on the specific thresholds we used to delineate the burn severity classes.

3.3. Effects of Burn Severity on Albedo

[23] Summer albedo followed similar trajectories as summer EVI for all burn severity classes stratified by dNBR values (Figures 6a–6d). Summer albedo was initially lower than prefire albedo, and the most severe burns had the lowest albedo 1 year after fire, although the reduction in summer albedo was less correlated with dNBR than with the reduction in EVI (Table 3). Summer albedo generally increased continuously for 8 years after fire, presumably as a consequence of increasing canopy cover [*Chambers and Chapin*, 2002; *Mack et al.*, 2008], the relatively high albedo of grasses and shrubs that establish early in succession [*Betts and Ball*, 1997], and the loss of black carbon coatings on

soil and woody debris [e.g., *Czimczik et al.*, 2003; *Kuzyakov et al.*, 2009]. The rate of albedo increase was largest in the most severely burned areas. Postfire albedo was generally higher than the prefire albedo climatology starting at between 2 and 3 years after fire (Figures 6e–6h). By 3–4 years after fire, summer albedo changes for the three severity classes had converged in all ecozones. By 5–8 years after-fire severe burns in the boreal shield and taiga shield had slightly higher summer albedo changes than did low-severity burns (student's t test, $p < 0.001$) (Figures 6e–6h). When burn severity was stratified by initial spring albedo change ($\Delta\alpha_0$) rather than dNBR, we found that 5–8 years after fire high-severity burns had summer albedo levels that were significantly larger than moderate- or low-severity burns (Figure S9 in Text S2).

[24] Areas burned most severely also had the largest postfire spring albedo increases, providing further evidence that negative radiative forcing may be amplified by increases in burn severity. An immediate increase in albedo was
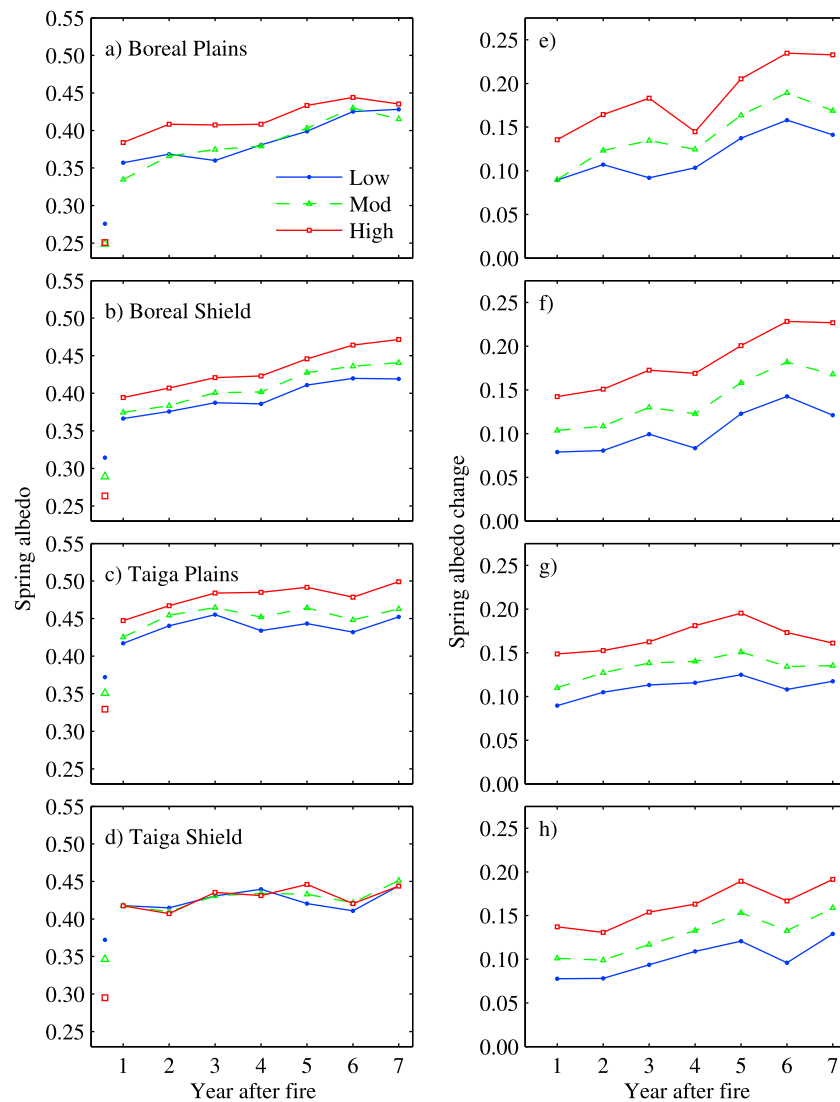
Figure 7. Same as Figure 6 but for spring albedo averaged for days of year 49–96.

observed in the spring following fire (Figures 7a–7d), and the magnitude of increase ($> = 0.07 \pm 0.04$) was much larger than that of the immediate summer albedo decrease ($< = 0.03 \pm 0.01$) (Table S3 in Text S1). The increases in postfire spring albedo became progressively larger with stand age from years 1–7, and may have been driven by a continued loss of branches from trees killed by the fire, increasing losses of standing dead boles [*Bond-Lamberty and Gower*, 2008] along with concurrent losses of black carbon coatings on these structural elements [e.g., *Czimczik et al.*, 2003; *Schmidt*, 2004]. The most severe burns had higher sustained spring albedo values and larger albedo trends for the first 7 years after fire (Figure 7). By 5–7 years after fire, the magnitude of albedo increases varied from 0.13 (± 0.06) for low-severity burns to 0.21 (± 0.06) for high-severity burns in boreal ecozones and from 0.11 (± 0.06) to 0.19 (± 0.06) in taiga zones. Thus, spring albedo increases were more than 60% larger in the most severely burned areas compared to low-severity burns (Table S3 in Text S1). The differences in time series of spring albedo increases between

moderate and high burn severity class were even larger when initial spring albedo change ($\Delta\alpha_0$) was used as the burn severity metric (Figure S10 in Text S2).

[25] The boreal zones had higher absolute spring albedo increase 5–7 years after fire for all 3 severity classes than did the taiga zones (Table S3 in Text S1). In terms of climate forcing, the cooling effects associated with these albedo increases would be further amplified by the higher incoming solar radiation in the south. However, the relative changes in albedo as a function of burn severity were similar in all ecozones. If burn severity intensified, (i.e., there was a widespread shift in severity from the low to the high class), the magnitude of albedo change in these area would increase similarly by approximately 0.06–0.08 (60%) for spring for all ecozones and by 0.001–0.004 in summer (Table S3 in Text S1).

[26] From the perspective of the burn severity continuum, the magnitude of albedo increase at 5–7 years after fire above prefire levels was positively correlated with dNBR, especially in spring (Figure 8 and Table 3). Spring albedo
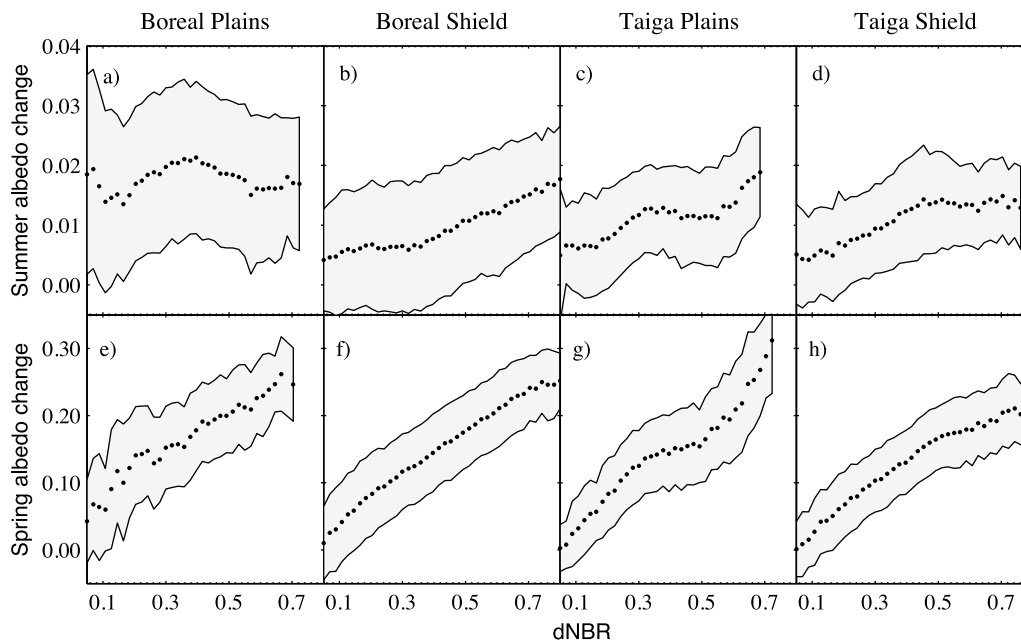
Figure 8. The influence of burn severity as measured by dNBR on (a–d) summer albedo change and (e–h) spring albedo change averaged 5–7 years after fire for each ecozone. The shaded areas represent the mean ± standard deviation of albedo change.

increased significantly as a linear function of dNBR for all ecozones. Areas of high dNBR values tended to have lower prefire spring albedo (Figure S11 in Text S2). These two opposite trends led to a pronounced increasing spring albedo change with intensification of fire severity (r > = 0.6) (Table 3). The slope from linear regressions of spring albedo change versus dNBR for all fire-affected pixels was highest in taiga plains (0.35 ± 0.01) and lowest in taiga shield (0.29 ± 0.00) (Table 3). Summer albedo changes showed much smaller but highly significant positive slopes (approximately 0.02 with units of albedo per unit of dNBR) for all ecozones (Figure 8 and Table 3). Decreases of prefire summer EVI, summer albedo, and spring albedo with increases in dNBR (Figures 4, 5, and S11) are consistent with the hypothesis that denser conifer forests may burn more severely than more open canopies, or forests that have a greater proportion of deciduous trees and shrubs. Deciduous trees and shrubs often have higher water content in leaves and thus a lower flammability [*Johnson*, 1992; *Cumming*, 2001]. These plant functional types also tend to have higher albedo and EVI values relative to conifers [*Betts and Ball*, 1997; *Huete et al.*, 2002]. Along a gradient of increasing $\Delta \alpha_0$, spring and summer albedo changes after fire also increased consistently in most ecozones (Figure S12 in Text S2 and Table S4 in Text S1).

3.4. Burn Severity Effects as a Function of Vegetation Type

[27] The most severe fires caused similar initial decreases in EVI (−0.16 ± 0.04) for all vegetation types, even though prefire EVI varied between vegetation types (Table S5 in Text S1). The absolute and relative reductions of EVI were the smallest for low-severity burns in broadleaf/mixed forests. By 5–7 years after fire, EVI was slightly higher than

prefire EVI by 0.02 for all severity classes in forest areas, while EVI did not exceed prefire values in taiga areas.

[28] Fire caused the largest spring albedo increase from prefire values in needleleaf forests 5–7 years after fire (i.e., albedo increased by 0.14 ± 0.06 and 0.22 ± 0.06 for low- and high-severity burns in needleleaf forests, compared with 0.11 ± 0.06 and 0.18 ± 0.06 in broadleaf/mixed forests) (Table S6 in Text S1). Increases in burn severity resulted in similar levels of spring albedo change (increases of approximately 0.06–0.08) from low- to high-severity burns for needleleaf forests, broadleaf and mixed forests, and shrublands vegetation types (Table S6 in Text S1). Albedo change had similar sensitivity to burn severity, with a correlation coefficient of greater than 0.58 between spring albedo change 5–7 years after fire and dNBR and a slope of 0.30 ± 0.02 (with units of albedo change per unit of dNBR) (Table S7 in Text S1).

4. Discussion

4.1. Implications of Burn Severity Changes for Fire-Climate Interactions

[29] Analysis of Alaska's fire record since the 1940s provides evidence for a recent increase in fire size and a recent seasonal shift to later fires [*Kasischke et al.*, 2010]. These changes in Alaskan fire regime have intensified burn severity, i.e., the depth of ground layer burning increases with fire size during early season burning and remains deeper throughout the fire season during large-fire years [*Turetsky et al.*, 2011a]. At a landscape scale, deeper burning during late season fires has resulted in more than a twofold increase in ecosystem carbon losses, with 6.15 ± 0.41 kg C m^{-2} for late season burning versus 2.95 ± 0.12 kg C m^{-2} for early season burning [*Turetsky et al.*, 2011a]. When *Turetsky*

et al. [2011a] included severity in a decadal-scale estimate of carbon losses from fires, they found that the mean flux increased by 75% during 1950–2009 compared to an emissions scenario using the same burned area but an average combustion rate.

[30] Our analysis indicates that burn severity also has a positive impact on postfire albedo increases during early succession in NABR, especially in spring, suggesting that a shift to more severe fire regimes would amplify the cooling effect associated with fire-induced albedo change. Further studies are needed to assess the impact of fire severity on the entire suite of radiative forcing agents associated with fire [*Bowman et al.*, 2009] with a goal of understanding climate feedbacks on multiple time scales. A key challenge in this regard will be to quantify carbon emissions, aerosol production, and albedo and surface energy change across burn severity gradients.

[31] Fire affects additional biophysical properties, including surface roughness, surface and boundary layer conductance, and surface temperature [e.g., *Baldocchi et al.*, 2000; *Bond-Lamberty et al.*, 2009; *Lee et al.*, 2011]. Field measurements on how these properties change during recovery [*Lee et al.*, 2011] as a function of burn severity are needed to understand the integrated effects of fire and its severity on climate. A useful next step is to examine the recovery pattern of postfire surface emissivity and skin temperature as a function of burn severity using MODIS land surface temperature product [*Wan*, 2008].

4.2. Do Burn Severity Effects on Surface Albedo Persist for Many Decades?

[32] Our results for early succession are consistent with other recent findings for intermediate-aged successional dynamics in the NABR [*Beck et al.*, 2011]. Spring albedo in high-severity burns was found to be higher than that for low-severity burns for 10–45 year old stands in interior Alaska, based on a severity metric derived from the seasonal timing and size of individual fires [*Beck et al.*, 2011]. This suggests that the sustained higher albedo in more severely burned areas we observed here during early succession most likely continues into intermediate aged stands. More quantitative evaluation of postfire trajectories at longer time scales will require integrating MODIS and Visible Infrared Imager Radiometer Suite (VIIRS) observations. VIIRS will extend the time series of land observations beyond MODIS era but significant challenges remain with respect to fusing these two sensors that have different pixel sizes and spectral sensitivities. A multi-decadal analysis of burn severity impacts could also be undertaken for individual fires or larger regions by constructing Landsat data stacks [e.g., *McMillan and Goulden*, 2008]. Here we observed that summer albedo exceeded prefire albedo by 5–8 years after fire, with albedo increases in high-severity burns larger than those in low-severity burns. Summer albedo change for the most severe burns may continue to exceed that in low-severity burns owing to the establishment of more deciduous trees in severely burned areas [e.g., *Mack et al.*, 2008]. We suspect that the impact of fire severity on spring and summer albedo increases further with stand age. Evidence supporting this hypothesis comes from trends in summer albedo observed by *Beck et al.* [2011] which show an increasing difference between the albedo in low- and high-severity burns for stands with ages between 10 and 30 years.

4.3. Does Spring Albedo Change Provide an Additional Satellite-Derived Index of Burn Severity in Boreal Forests?

[33] dNBR is a widely used index for burn severity [*French et al.*, 2008]. It quantifies the contrast between decreases of NIR reflectance associated with the loss of vegetation and increases of SW-IR reflectance from changes in the soil moisture regime. Here we showed that spring albedo change immediately after fire ($\Delta\alpha_0$) was highly correlated with summer dNBR measurements in all ecozones. Snow is common in early spring in most boreal and tundra regions, and spring albedo is especially sensitive to the presence of leaves and live or dead stems and the associated snow exposure. A greater consumption of soil organic matter in high-severity burns may be correlated with an increased combustion of canopy components and with an increased number of snags that fall over. Field investigations along burn severity gradients, perhaps using higher-resolution Landsat observations, are needed to further explore the potential of this index.

[34] Some of the drivers of uncertainty in dNBR and $\Delta\alpha_0$ are probably mostly independent, suggesting that their combined use may offer complementary perspectives of severity. Summer drought before or after fire affects dNBR, for example, while year-to-year variability in snow cover may affect $\Delta\alpha_0$. Both measures of severity are potentially sensitive to changes in climate over a period of decades. Snow cover decreases are expected to accelerate over the 21st century [*Kuang and Yung*, 2000; *Dye*, 2002; *Euskirchen et al.*, 2006], thus influencing the long-term stability of severity measures derived from $\Delta\alpha_0$. Similarly, concurrent warming may influence species composition and the growth rate of colonizers in burned areas after fire, thus influencing both postfire NBR and prefire NBR.

[35] Use of $\Delta\alpha_0$ as a metric of burn severity is probably most effective in forested regions. Peatlands cover about 12% of Canada's land area, and often have a well-established tree or shrub layer in Western Canada [*Turetsky et al.*, 2011b]. The sensitivity of $\Delta\alpha_0$ to burn severity would be expected to lower in peatland and tundra regions because of reduced fire effects on areas with scattered or no trees [*Chambers et al.*, 2005]. In Alaskan boreal forests, there is some evidence that burn severity varies with fire size, topography, and season [*Beck et al.*, 2011]. It would be interesting to investigate how well the season and size of burning represent burn severity at the burn perimeter spatial scale across different ecoregions in Canada.

4.4. Why Do More Severe Fires Show More Rapid Postfire EVI Increases?

[36] More rapid postfire increases in EVI for more severe burns are likely a combination of several factors. An increase in combustion of surface organic material in severe burns exposes more mineral soils, which favors the growth of herbaceous species and deciduous trees [*Johnstone et al.*, 2010]. Herbaceous cover [*Johnstone and Chapin*, 2006] and the aboveground biomass of aspen seedlings [*Johnstone*

and Kasischke, 2005] respond positively to increased burn severity. Soil moisture stress, a primary limitation on the establishment of deciduous species, is reduced on mineral soil by increased wicking from subsurface layers and decreased temperature rise associated with increased thermal capacity [*Johnstone and Chapin*, 2006]. Deciduous broadleaf trees have higher NIR reflectance and EVIs than evergreen conifers [*Huete et al.*, 2002; *Roberts et al.*, 2004].

[37] EVI also may be more sensitive to small changes in vegetation cover at lower EVI values [*Choudhury et al.*, 1994; *Baret et al.*, 1995]. Thus, the nonlinearity between EVI and vegetation cover also may contribute to more rapid EVI recovery for high-severity burns, which had the lowest EVI during the first year after fire. An important related question is whether the EVI differences between low- and high-severity fires observed here persist during intermediate stages of succession. *Goetz et al.* [2006] show that NDVI is often higher than prefire levels between 5 and 15 years after fires across Canada.

[38] Future work is needed to test if EVI differences among different burn severity classes, which are most distinct for the burn severity metric based on the initial spring albedo change, are maintained through time. EVI is well correlated with CO_2 uptake [e.g., *McMillan and Goulden*, 2008], and the rapid recovery of CO_2 uptake in severely burned areas may amplify the negative forcing associated with fire-induced albedo change. This underscores the need for more quantitative analysis of the relationship between burn severity and all of the factors that may contribute to radiative forcing.

5. Conclusions

[39] We quantified the influence of burn severity on vegetation recovery and albedo change within the first decade after fire in 4 Canadian ecozones. We derived dNBR and initial spring albedo change from MODIS 500 m albedo as measures of burn severity. These metrics were correlated with one another and were closely related to initial changes in vegetation cover as measured using EVI. Boreal fire removes vegetation and changes species composition [*Goulden et al.*, 2011]. Deciduous grasses and shrubs that establish early in succession usually have relatively high albedo both in summer, due to brighter leaf and canopy reflectances, and in winter, due to more snow exposure [*Betts and Ball*, 1997]. We found that high-severity burns had the largest decreases in summer EVI and albedo and the largest increases in spring albedo in the first year after fire. EVI in areas with varying levels of burn severity had mostly converged by 5–8 years after fire, due to more rapid vegetation recovery in more severely burned areas. In contrast, the higher spring albedo and larger albedo increases in areas that had burned more severely were sustained for at least 7 years after fire. A shift from low- to high-severity fires led to approximately 60% amplification of the postfire spring albedo increase. Spring albedo change was well correlated with dNBR (and $\Delta\alpha_0$) in all ecozones and for all vegetation types, with correlation coefficients greater than 0.61 and slopes greater than 0.29 ($\pm$0.01) per unit change of dNBR. Our study indicates that increases in fire severity would amplify the negative radiative forcing associated with fire-induced albedo change.

This may partly offset the positive feedback effect of warming caused by increasing carbon losses under an intensifying fire regime.

References

Allen, J. L., and B. Sorbel (2008), Assessing the differenced Normalized Burn Ratio's ability to map burn severity in the boreal forest and tundra ecosystems of Alaska's national parks, *Int. J. Wildland Fire*, 17(4), 463–475, doi:10.1071/WF08034.

Amiro, B. D., B. J. Stocks, M. E. Alexander, M. D. Flannigan, and B. M. Wotton (2001), Fire, climate change, carbon and fuel management in the Canadian boreal forest, *Int. J. Wildland Fire*, 10(4), 405–413, doi:10.1071/WF01038.

Amiro, B. D., et al. (2006), The effect of postfire stand age on the boreal forest energy balance, *Agric. For. Meteorol.*, 140(1–4), 41–50, doi:10.1016/j.agrformet.2006.02.014.

Baldocchi, D., F. M. Kelliher, T. A. Black, and P. Jarvis (2000), Climate and vegetation controls on boreal zone energy exchange, *Global Change Biol.*, 6, 69–83, doi:10.1046/j.1365-2486.2000.06014.x.

Balshi, M. S., et al. (2007), The role of historical fire disturbance in the carbon dynamics of the pan-boreal region: A process-based analysis, *J. Geophys. Res.*, 112, G02029, doi:10.1029/2006JG000380.

Balshi, M. S., A. D. McGuire, P. Duffy, M. Flannigan, D. W. Kicklighter, and J. Melillo (2009), Vulnerability of carbon storage in North American boreal forests to wildfires during the 21st century, *Global Change Biol.*, 15, 1491–1510, doi:10.1111/j.1365-2486.2009.01877.x.

Baret, F., J. G. P. W. Clevers, and M. D. Steven (1995), The robustness of canopy gap fraction estimates from red and near-infrared reflectances: A comparison of approaches, *Remote Sens. Environ.*, 54(2), 141–151, doi:10.1016/0034-4257(95)00136-O.

Barrett, K., E. S. Kasischke, A. D. McGuire, M. R. Turetsky, and E. S. Kane (2010), Modeling fire severity in black spruce stands in the Alaskan boreal forest using spectral and non-spectral geospatial data, *Remote Sens. Environ.*, 114(7), 1494–1503, doi:10.1016/j.rse.2010.02.001.

Beck, P. S. A., S. J. Goetz, M. C. Mack, H. D. Alexander, Y. Jin, J. T. Randerson, and M. M. Loranty (2011), The impacts and implications of an intensifying fire regime on Alaskan boreal forest composition and albedo, *Global Change Biol.*, 17, 2853–2866, doi:10.1111/j.1365-2486.2011.02412.x.

Betts, A. K., and J. H. Ball (1997), Albedo over the boreal forest, *J. Geophys. Res.*, 102(D24), 28,901–28,909, doi:10.1029/96JD03876.

Bonan, G. B., D. Pollard, and S. L. Thompson (1992), Effects of boreal forest vegetation on global climate, *Nature*, 359(6397), 716–718, doi:10.1038/359716a0.

Bond-Lamberty, B., and S. T. Gower (2008), Decomposition and fragmentation of coarse woody debris: Re-visiting a boreal black spruce chronosequence, *Ecosystems*, 11(6), 831–840, doi:10.1007/s10021-008-9163-y.

Bond-Lamberty, B., S. D. Peckham, D. E. Ahl, and S. T. Gower (2007), Fire as the dominant driver of central Canadian boreal forest carbon balance, *Nature*, 450(7166), 89–92, doi:10.1038/nature06272.

Bond-Lamberty, B., S. D. Peckham, S. T. Gower, and B. Ewers (2009), Effects of fire on regional evapotranspiration in the central Canadian boreal forest, *Global Change Biol.*, 15, 1242–1254, doi:10.1111/j.1365-2486.2008.01776.x.

Bowman, M. J. S., et al. (2009), Fire in the Earth system, *Science*, 324(5926), 481–484, doi:10.1126/science.1163886.

Chambers, S. D., and F. S. Chapin III (2002), Fire effects on surface-atmosphere energy exchange in Alaskan black spruce ecosystems: Implications for feedbacks to regional climate, *J. Geophys. Res.*, 107, 8145, doi:10.1029/2001JD000530. [Printed 108(D1), 2003.]

Chambers, S. D., J. Beringer, J. T. Randerson, and F. S. Chapin III (2005), Fire effects on net radiation and energy partitioning: Contrasting responses of tundra and boreal forest ecosystems, *J. Geophys. Res.*, 110, D09106, doi:10.1029/2004JD005299.

Choudhury, B. J., N. U. Ahmed, S. B. Idso, R. J. Reginato, and C. S. T. Daughtry (1994), Relations between evaporation coefficients and vegetation indexes studied by model simulations, *Remote Sens. Environ.*, 50(1), 1–17, doi:10.1016/0034-4257(94)90090-6.

Conard, S. G., A. I. Sukhinin, B. J. Stocks, D. R. Cahoon, E. P. Davidenko, and G. A. Ivanova (2002), Determining effects of area burned and fire severity on carbon cycling and emissions in Siberia, *Clim. Change*, *55*, 197–211, doi:10.1023/A:1020207710195.

Cumming, S. G. (2001), Forest type and wildfire in the alberta boreal mixedwood: What do fires burn?, *Ecol. Appl.*, *11*(1), 97–110, doi:10.1890/1051-0761(2001)011[0097:FTAWIT]2.0.CO;2.

Czimczik, C. I., C. M. Preston, M. W. I. Schmidt, and E.-D. Schulze (2003), How surface fire in Siberian Scots pine forests affects soil organic carbon in the forest floor: Stocks, molecular structure, and conversion to black carbon (charcoal), *Global Biogeochem. Cycles*, *17*(1), 1020, doi:10.1029/2002GB001956.

de Groot, W. J., J. M. Pritchard, and T. J. Lynham (2009), Forest floor fuel consumption and carbon emissions in Canadian boreal forest fires, *Can. J. For. Res.*, *39*(2), 367–382, doi:10.1139/X08-192.

Duffy, P. A., J. Epting, J. M. Graham, T. S. Rupp, and A. D. McGuire (2007), Analysis of Alaskan burn severity patterns using remotely sensed data, *Int. J. Wildland Fire*, *16*(3), 277–284, doi:10.1071/WF06034.

Dye, D. G. (2002), Variability and trends in the annual snow-cover cycle in Northern Hemisphere land areas, 1972–2000, *Hydrol. Processes*, *16*(15), 3065–3077, doi:10.1002/hyp.1089.

Epting, J., D. Verbyla, and B. Sorbel (2005), Evaluation of remotely sensed indices for assessing burn severity in interior Alaska using Landsat TM and ETM+, *Remote Sens. Environ.*, *96*(3–4), 328–339, doi:10.1016/j.rse.2005.03.002.

Eugster, W., et al. (2000), Land-atmosphere energy exchange in Arctic tundra and boreal forest: Available data and feedbacks to climate, *Global Change Biol.*, *6*, 84–115, doi:10.1046/j.1365-2486.2000.06015.x.

Euskirchen, E. S., et al. (2006), Importance of recent shifts in soil thermal dynamics on growing season length, productivity, and carbon sequestration in terrestrial high-latitude ecosystems, *Global Change Biol.*, *12*, 731–750, doi:10.1111/j.1365-2486.2006.01113.x.

Euskirchen, E. S., A. D. McGuire, T. S. Rupp, F. S. Chapin III, and J. E. Walsh (2009), Projected changes in atmospheric heating due to changes in fire disturbance and the snow season in the western Arctic, 2003–2100, *J. Geophys. Res.*, *114*, G04022, doi:10.1029/2009JG001095.

Flanner, M. G., C. S. Zender, J. T. Randerson, and P. J. Rasch (2007), Present-day climate forcing and response from black carbon in snow, *J. Geophys. Res.*, *112*, D11202, doi:10.1029/2006JD008003.

Flannigan, M. D., B. J. Stocks, and B. M. Wotton (2000), Climate change and forest fires, *Sci. Total Environ.*, *262*(3), 221–229, doi:10.1016/S0048-9697(00)00524-6.

Flannigan, M. D., K. A. Logan, B. D. Amiro, W. R. Skinner, and B. J. Stocks (2005), Future area burned in Canada, *Clim. Change*, *72*, 1–16, doi:10.1007/s10584-005-5935-y.

French, N. H. F., E. S. Kasischke, R. J. Hall, K. A. Murphy, D. L. Verbyla, E. E. Hoy, and J. L. Allen (2008), Using Landsat data to assess fire and burn severity in the North American boreal forest region: An overview and summary of results, *Int. J. Wildland Fire*, *17*(4), 443–462, doi:10.1071/WF08007.

Friedl, M. A., et al. (2002), Global land cover mapping from MODIS: Algorithms and early results, *Remote Sens. Environ.*, *83*(1–2), 287–302, doi:10.1016/S0034-4257(02)00078-0.

Friedl, M. A., D. Sulla-Menashe, B. Tan, A. Schneider, N. Ramankutty, A. Sibley, and X. M. Huang (2010), MODIS Collection 5 global land cover: Algorithm refinements and characterization of new datasets, *Remote Sens. Environ.*, *114*(1), 168–182, doi:10.1016/j.rse.2009.08.016.

Gillett, N. P., A. J. Weaver, F. W. Zwiers, and M. D. Flannigan (2004), Detecting the effect of climate change on Canadian forest fires, *Geophys. Res. Lett.*, *31*, L18211, doi:10.1029/2004GL020876.

Goetz, S. J., and S. D. Prince (1998), Variability in carbon exchange and light utilization among boreal forest stands: Implications for remote sensing of net primary production, *Can. J. For. Res.*, *28*(3), 375–389.

Goetz, S. J., G. Fiske, and A. Bunn (2006), Using satellite time series data sets to analyze fire disturbance and recovery in the Canadian boreal forest, *Remote Sens. Environ.*, *101*(3), 352–365, doi:10.1016/j.rse.2006.01.011.

Goetz, S. J., M. C. Mack, K. R. Gurney, J. T. Randerson, and R. A. Houghton (2007), Ecosystem responses to recent climate change and fire disturbance at northern high latitudes: Observations and model results contrasting northern Eurasia and North America [online], *Environ. Res. Lett.*, *2*, 045031, doi:10.1088/1748-9326/2/4/045031.

Goulden, M. L., A. M. S. McMillan, G. C. Winston, A. V. Rocha, K. L. Manies, J. W. Harden, and B. P. Bond-Lamberty (2011), Patterns of NPP, GPP, respiration, and NEP during boreal forest succession, *Global Change Biol.*, *17*, 855–871, doi:10.1111/j.1365-2486.2010.02274.x.

Hall, R. J., J. T. Freeburn, W. J. de Groot, J. M. Pritchard, T. J. Lynham, and R. Landry (2008), Remote sensing of burn severity: Experience from western Canada boreal fires, *Int. J. Wildland Fire*, *17*(4), 476–489, doi:10.1071/WF08013.

Harden, J. W., S. E. Trumbore, B. J. Stocks, A. Hirsch, S. T. Gower, K. P. O'Neill, and E. S. Kasischke (2000), The role of fire in the boreal carbon budget, *Global Change Biol.*, *6*, 174–184, doi:10.1046/j.1365-2486.2000.06019.x.

Hoy, E. E., N. H. F. French, M. R. Turetsky, S. N. Trigg, and E. S. Kasischke (2008), Evaluating the potential of Landsat TM/ETM+ imagery for assessing fire severity in Alaskan black spruce forests, *Int. J. Wildland Fire*, *17*(4), 500–514, doi:10.1071/WF08107.

Huete, A., K. Didan, T. Miura, E. P. Rodriguez, X. Gao, and L. G. Ferreira (2002), Overview of the radiometric and biophysical performance of the MODIS vegetation indices, *Remote Sens. Environ.*, *83*(1–2), 195–213, doi:10.1016/S0034-4257(02)00096-2.

Jin, Y., C. B. Schaaf, F. Gao, X. Li, A. H. Strahler, X. Zeng, and R. E. Dickinson (2002), How does snow impact the albedo of vegetated land surfaces as analyzed with MODIS data?, *Geophys. Res. Lett.*, *29*(10), 1374, doi:10.1029/2001GL014132.

Jin, Y. F., C. B. Schaaf, C. E. Woodcock, F. Gao, X. Li, A. H. Strahler, W. Lucht, and S. Liang (2003), Consistency of MODIS surface bidirectional reflectance distribution function and albedo retrievals: 2. Validation, *J. Geophys. Res.*, *108*(D5), 4159, doi:10.1029/2002JD002804.

Johnson, E. A. (1992), *Fire and Vegetation Dynamics: Studies From the North American Boreal Forest*, Cambridge Univ. Press, Cambridge, U. K., doi:10.1017/CBO9780511623516.

Johnson, E. A., K. Miyanishi, and J. M. H. Weir (1998), Wildfires in the western Canadian boreal forest: Landscape patterns and ecosystem management, *J. Veg. Sci.*, *9*(4), 603–610, doi:10.2307/3237276.

Johnstone, J., and F. Chapin (2006), Effects of soil burn severity on postfire tree recruitment in boreal forest, *Ecosystems*, *9*(1), 14–31, doi:10.1007/s10021-004-0042-x.

Johnstone, J. F., and E. S. Kasischke (2005), Stand-level effects of soil burn severity on postfire regeneration in a recently burned black spruce forest, *Can. J. For. Res.*, *35*(9), 2151–2163, doi:10.1139/x05-087.

Johnstone, J. F., F. S. Chapin III, J. Foote, S. Kemmett, K. Price, and L. Viereck (2004), Decadal observations of tree regeneration following fire in boreal forests, *Can. J. For. Res.*, *34*(2), 267–273, doi:10.1139/x03-183.

Johnstone, J. F., T. N. Hollingsworth, F. S. Chapin III, and M. C. Mack (2010), Changes in fire regime break the legacy lock on successional trajectories in Alaskan boreal forest, *Global Change Biol.*, *16*, 1281–1295, doi:10.1111/j.1365-2486.2009.02051.x.

Kasischke, E. S., and M. R. Turetsky (2006), Recent changes in the fire regime across the North American boreal region—Spatial and temporal patterns of burning across Canada and Alaska, *Geophys. Res. Lett.*, *33*, L09703, doi:10.1029/2006GL025677.

Kasischke, E. S., K. P. O'Neill, N. H. F. French, and L. L. Bourgeau-Chavez (2000), Controls on patterns of biomass burning in Alaskan boreal forests, in *Fire, Climate Change, and Carbon Cycling in the Boreal Forest*, edited by E. S. Kasischke and B. J. Stocks, pp. 173–196, Springer, New York.

Kasischke, E. S., M. R. Turetsky, R. D. Ottmar, N. H. F. French, E. E. Hoy, and E. S. Kane (2008), Evaluation of the composite burn index for assessing fire severity in Alaskan black spruce forests, *Int. J. Wildland Fire*, *17*(4), 515–526, doi:10.1071/WF08002.

Kasischke, E. S., et al. (2010), Alaska's changing fire regime—Implications for the vulnerability of its boreal forests, *Can. J. For. Res.*, *40*(7), 1313–1324, doi:10.1139/X10-098.

Key, C. H., and N. C. Benson (2006), Landscape assessment: Sampling and analysis methods, in *FIREMON: Fire Effects Monitoring and Inventory System*, edited by D. C. Lutes et al., *Gen. Tech. Rep. RMRS-GTR-164-CD*, pp. LA1–LA51, Rocky Mt. Res. Stn., U.S. For. Serv., U.S. Dep. of Agric., Fort Collins, Colo.

Krawchuk, M. A., and S. G. Cumming (2011), Effects of biotic feedback and harvest management on boreal forest fire activity under climate change, *Ecol. Appl.*, *21*(1), 122–136, doi:10.1890/09-2004.1.

Kuang, Z. M., and Y. L. Yung (2000), Observed albedo decrease related to the spring snow retreat, *Geophys. Res. Lett.*, *27*(9), 1299–1302, doi:10.1029/1999GL011116.

Kurz, W. A., and M. J. Apps (1999), A 70-year retrospective analysis of carbon fluxes in the Canadian forest sector, *Ecol. Appl.*, *9*(2), 526–547, doi:10.1890/1051-0761(1999)009[0526:AYRAOC]2.0.CO;2.

Kuzyakov, Y., I. Subbotina, H. Chen, I. Bogomolova, and X. L. Xu (2009), Black carbon decomposition and incorporation into soil microbial biomass estimated by ^{14}C labeling, *Soil Biol. Biochem.*, *41*(2), 210–219, doi:10.1016/j.soilbio.2008.10.016.

Lavoie, L., and L. Sirois (1998), Vegetation changes caused by recent fires in the northern boreal forest of eastern Canada, *J. Veg. Sci.*, *9*(4), 483–492, doi:10.2307/3237263.

Lee, X., et al. (2011), Observed increase in local cooling effect of deforestation at higher latitudes, *Nature*, *479*, 384–387, doi:10.1038/nature10588.

Liu, H. P., J. T. Randerson, J. Lindfors, and F. S. Chapin III (2005), Changes in the surface energy budget after fire in boreal ecosystems of interior Alaska: An annual perspective, *J. Geophys. Res.*, *110*, D13101, doi:10.1029/2004JD005158.

Lyons, E. A., Y. F. Jin, and J. T. Randerson (2008), Changes in surface albedo after fire in boreal forest ecosystems of interior Alaska assessed using MODIS satellite observations, *J. Geophys. Res.*, *113*, G02012, doi:10.1029/2007JG000606.

Mack, M. C., K. K. Treseder, K. L. Manies, J. W. Harden, E. A. G. Schuur, J. G. Vogel, J. T. Randerson, and F. S. Chapin (2008), Recovery of aboveground plant biomass and productivity after fire in mesic and dry black spruce forests of interior Alaska, *Ecosystems*, *11*(2), 209–225, doi:10.1007/s10021-007-9117-9.

Marshall, I. B., P. H. Schut, and M. Ballard (1999), A national ecological framework for Canada: Attribute data report [online], Cent. for Land and Biol. Resour. Res., Agric. and Agri-Food Can., Ottawa. [Available at http://sis.agr.gc.ca/cansis/nsdb/ecostrat/1999report/intro.html.]

McGuire, A. D. et al. (2004), Land cover disturbances and feedbacks to the climate system in Canada and Alaska, in *Land Change Science: Observing, Monitoring, and Understanding Trajectories of Change on the Earth's Surface, Remote Sens. Digital Image Process.*, vol. 6, edited by G. Gutman et al., pp. 139–161, Kluwer Acad., Dordrecht, Netherlands, doi:10.1007/978-1-4020-2562-4_9.

McMillan, A. M. S., and M. L. Goulden (2008), Age-dependent variation in the biophysical properties of boreal forests, *Global Biogeochem. Cycles*, *22*, GB2023, doi:10.1029/2007GB003038.

Miyanishi, K., and E. A. Johnson (2002), Process and patterns of duff consumption in the mixedwood boreal forest, *Can. J. For. Res.*, *32*(7), 1285–1295, doi:10.1139/x02-051.

Rahman, A. F., D. A. Sims, V. D. Cordova, and B. Z. El-Masri (2005), Potential of MODIS EVI and surface temperature for directly estimating per-pixel ecosystem C fluxes, *Geophys. Res. Lett.*, *32*, L19404, doi:10.1029/2005GL024127.

Randerson, J. T., et al. (2006), The impact of boreal forest fire on climate warming, *Science*, *314*(5802), 1130–1132, doi:10.1126/science.1132075.

Roberts, D. A., S. L. Ustin, S. Ogunjemiyo, J. Greenberg, S. Z. Dobrowski, J. Q. Chen, and T. M. Hinckley (2004), Spectral and structural measures of northwest forest vegetation at leaf to landscape scales, *Ecosystems*, *7*(5), 545–562, doi:10.1007/s10021-004-0144-5.

Rocha, A. V., and G. R. Shaver (2011), Postfire energy exchange in arctic tundra: The importance and climatic implications of burn severity, *Global Change Biol.*, *17*, 2831–2841, doi:10.1111/j.1365-2486.2011.02441.x.

Schaaf, C. B., et al. (2002), First operational BRDF, albedo nadir reflectance products from MODIS, *Remote Sens. Environ.*, *83*(1–2), 135–148, doi:10.1016/S0034-4257(02)00091-3.

Schmidt, M. W. I. (2004), Biogeochemistry: Carbon budget in the black, *Nature*, *427*, 305–307, doi:10.1038/427305a.

Shenoy, A., J. F. Johnstone, E. S. Kasischke, and K. Kielland (2011), Persistent effects of fire severity on early successional forests in interior Alaska, *For. Ecol. Manage.*, *261*(3), 381–390, doi:10.1016/j.foreco.2010.10.021.

Sims, D. A., et al. (2006), On the use of MODIS EVI to assess gross primary productivity of North American ecosystems, *J. Geophys. Res.*, *111*, G04015, doi:10.1029/2006JG000162.

Soverel, N. O., D. D. B. Perrakis, and N. C. Coops (2010), Estimating burn severity from Landsat dNBR and RdNBR indices across western Canada, *Remote Sens. Environ.*, *114*(9), 1896–1909, doi:10.1016/j.rse.2010.03.013.

Stocks, B. J., et al. (2002), Large forest fires in Canada, 1959–1997, *J. Geophys. Res.*, *107*, 8149, doi:10.1029/2001JD000484. [Printed *108*(D1), 2003.]

Tucker, C. J., and P. J. Sellers (1986), Satellite remote sensing of primary production, *Int. J. Remote Sens.*, *7*(11), 1395–1416, doi:10.1080/01431168608948944.

Turetsky, M. R., E. S. Kane, J. W. Harden, R. D. Ottmar, K. L. Manies, E. Hoy, and E. S. Kasischke (2011a), Recent acceleration of biomass burning and carbon losses in Alaskan forests and peatlands, *Nat. Geosci.*, *4*(1), 27–31, doi:10.1038/ngeo1027.

Turetsky, M. R., W. F. Donahue, and B. W. Benscoter (2011b), Experimental drying intensifies burning and carbon losses in a northern peatland, *Nat. Commun.*, *2*, 514, doi:10.1038/ncomms1523.

Wan, Z. (2008), New refinements and validation of the MODIS land-surface temperature/emissivity products, *Remote Sens. Environ.*, *112*(1), 59–74, doi:10.1016/j.rse.2006.06.026.

Wotton, B. M., and M. D. Flannigan (1993), Length of the fire season in a changing climate, *For. Chron.*, *69*(2), 187–192.

Xiao, X. M., D. Hollinger, J. Aber, M. Goltz, E. A. Davidson, Q. Zhang, and B. Moore III (2004a), Satellite-based modeling of gross primary production in an evergreen needleleaf forest, *Remote Sens. Environ.*, *89*(4), 519–534, doi:10.1016/j.rse.2003.11.008.

Xiao, X. M., Q. Zhang, B. Braswell, S. Urbanski, S. Boles, S. Wofsy, M. Berrien, B. Moore III, and D. Ojima (2004b), Modeling gross primary production of temperate deciduous broadleaf forest using satellite images and climate data, *Remote Sens. Environ.*, *91*(2), 256–270, doi:10.1016/j.rse.2004.03.010.

Yi, S. H., et al. (2009), Interactions between soil thermal and hydrological dynamics in the response of Alaska ecosystems to fire disturbance, *J. Geophys. Res.*, *114*, G02015, doi:10.1029/2008JG000841.

Zhuang, Q. L., J. M. Melillo, M. C. Sarofim, D. W. Kicklighter, A. D. McGuire, B. S. Felzer, A. Sokolov, R. G. Prinn, P. A. Steudler, and S. M. Hu (2006), CO_2 and CH_4 exchanges between land ecosystems and the atmosphere in northern high latitudes over the 21st century, *Geophys. Res. Lett.*, *33*, L17403, doi:10.1029/2006GL026972.

P. S. A. Beck, S. J. Goetz, and M. M. Loranty, Woods Hole Research Center, 149 Woods Hole Rd., Falmouth, MA 02540, USA.

M. L. Goulden, Y. Jin, and J. T. Randerson, Department of Earth System Science, University of California, Irvine, CA 92697, USA. (yufang@uci.edu)